



# ***STH-net*: a soil monitoring network for process-based hydrological modelling from the pedon to the hillslope scale**

Edoardo Martini<sup>1,2</sup>, Matteo Bauckholt<sup>2</sup>, Simon Kögler<sup>a</sup>, Manuel Kreck<sup>2</sup>, Kurt Roth<sup>1</sup>, Ulrike Werban<sup>2</sup>, Ute Wollschläger<sup>3</sup>, and Steffen Zacharias<sup>2</sup>

<sup>1</sup>Institute of Environmental Physics, Heidelberg University, Heidelberg, 69120, Germany

<sup>2</sup>Department of Monitoring and Exploration Technologies, Helmholtz Centre for Environmental Research GmbH – UFZ, Leipzig, 04318, Germany

<sup>3</sup>Department of Soil System Science, Helmholtz Centre for Environmental Research GmbH – UFZ, Halle (Saale), 06120, Germany

<sup>a</sup>formerly at: Department of Monitoring and Exploration Technologies, Helmholtz Centre for Environmental Research GmbH – UFZ, Leipzig, 04318, Germany

**Correspondence:** Edoardo Martini (emartini@iup.uni-heidelberg.de)

Received: 27 November 2020 – Discussion started: 5 January 2021

Revised: 13 April 2021 – Accepted: 5 May 2021 – Published: 4 June 2021

**Abstract.** The *Schärfertal Hillslope* site is part of the TERENO Harz/Central German Lowland Observatory, and its soil water dynamics are being monitored intensively as part of an integrated, long-term, multi-scale, and multi-temporal research framework linking hydrological, pedological, atmospheric, and biodiversity-related research to investigate the influences of climate and land use change on the terrestrial system. Here, a new soil monitoring network, indicated as *STH-net*, has been recently implemented to provide high-resolution data about the most relevant hydrological variables and local soil properties. The monitoring network is spatially optimized, based on previous knowledge from soil mapping and soil moisture monitoring, in order to capture the spatial variability in soil properties and soil water dynamics along a catena across the site as well as in depth. The *STH-net* comprises eight stations instrumented with time-domain reflectometry (TDR) probes, soil temperature probes, and monitoring wells. Furthermore, a weather station provides data about the meteorological variables. A detailed soil characterization exists for locations where the TDR probes are installed. All data have been measured at a 10 min interval since 1 January 2019. The *STH-net* is intended to provide scientists with data needed for developing and testing modelling approaches in the context of vadose-zone hydrology at spatial scales ranging from the pedon to the hillslope. The data are available from the EUDAT portal (<https://doi.org/10.23728/b2share.82818db7be054f5eb921d386a0bcaa74>, Martini et al., 2020).

## **1 Introduction**

Soils are embedded in the environment, coupled to vegetation and atmosphere at the land surface and to groundwater at its lower end. This coupling gives rise to a suite of physical, chemical, and biological dynamics, most of which are highly non-linear and varying in time and space. Soils provide crucial ecosystem functions such as water storage and filtering, food and other biomass production, recycling

of carbon and nutrients, biological habitat and gene pool, physical and cultural heritage, source of raw materials, and platforms for human life (United Nations, 2014; Vereecken et al., 2016). Soils are widely distributed on the earth's surface. Flow and transport processes in unsaturated soils occur predominantly in the vertical direction, with the gravity force playing a major role, as abrupt changes in soil properties due to soil horizons and layers are typically more significant than those in the lateral direction and because of the strong cou-

pling between soil, vegetation, and atmosphere. Therefore, despite the relevance of soils for global phenomena, the relevant soil processes are rather local. Here, one aspect that complicates the picture is the heterogeneity of soil properties. Another one is the non-linearity of soil processes. In order to effectively address this complexity, state-of-the-art experimental approaches must be coupled to numerical models for the comprehensive representation of the system properties, states, and fluxes so that the hydrological system can be better understood.

Recently, Vogel (2019) provided a comprehensive discussion about the scales and scaling issues in the context of soil hydrological research and noted the need for looking at small-scale soil properties (i.e. at the pedon scale, at which soil physics is capable of describing states and fluxes with sufficient accuracy) as a necessary step towards understanding and summarizing the processes at larger scales. In this respect, the author stresses the need for a two-step approach based on the accurate description of the soil water dynamics at the pedon scale and accounting for the spatial patterns of functional soil types that constitute the landscape, including the vertical stratification of soil hydraulic properties and structural attributes. However, the author remarks that high-resolution measurements of the relevant states and properties cannot be achieved at the larger scale (i.e. catchment, the typical scale of application of hydrological research). In this context, the intermediate scale of hillslopes is crucial for linking the detailed process understanding to larger-scale dynamics, recognizing hillslopes as key landscape features that organize water availability on land (Fan et al., 2019). In this respect, coupling state-of-the-art hydrological modelling approaches with high-resolution subsurface characterization can lead to an accurate quantification of the soil water dynamics in the vadose zone (Vereecken et al., 2015).

The physical description of the small-scale water movement through the soil's porous structure is typically achieved using the Richards equation. However, a detailed description of the material properties is needed and cannot be fully resolved by direct sampling. Thus, inverse modelling can be a powerful tool for the estimation of the soil hydraulic parameters (e.g. Vrugt et al., 2008), including the recent developments in data assimilation approaches (e.g. Bauser et al., 2016, 2020; Botto et al., 2018). These require dense (in the direction of the dominant flow, typically orthogonal to the soil surface) measurements of soil water content with high temporal resolution and of high quality. Furthermore, in situ sensors can experience all the processes affecting the measured state variables in their natural environment (Wollschläger et al., 2009), which is an important advantage with respect to sample-based determinations from the laboratory.

The performances of hydrological models can be improved by various measured data with high spatial and temporal resolution (Clark et al., 2017). Bronstert (1999) highlighted the importance of linking experimental knowledge to

the experience gained from numerical modelling applications as a very valuable synergistic combination. Technological advances in our ability to measure soil hydrological states efficiently at the hillslope scale and beyond are one possible way to gain the much-needed improved understanding of processes that challenge the comprehensive understanding of field-scale hydrology.

In the research framework of the TERENO Harz/Central German Lowland Observatory, the *Schäferfetal Hillslope* represents a benchmark site for developing and testing the integration of state-of-the-art monitoring techniques with advanced modelling approaches. This offers the opportunity to gain a more detailed understanding of processes and to quantify and predict water and matter fluxes at nested spatial scales in the context of climate and land use change. Specifically, the approach followed at the site accounts for the soil spatial variability through detailed soil mapping and is designed to provide in situ data with high-temporal-resolution and dense coverage in the vertical direction about the soil water dynamics in the vadose zone and of its boundary conditions. With this design tailored to the needs of vadose zone modelling, we aim to provide physical models with ideally all the data needed for quantifying and predicting the soil water fluxes at spatial scales ranging from the pedon to the hillslope scale, with important implications in terms of methodological advance and process understanding for catchment-scale processes.

Here, we present the first 21 months of the comprehensive data set measured by the monitoring network *STH-net*, recently implemented at the Schäferfetal Hillslope site, part of an intensive hydrological observatory. The data set includes hourly time series of the meteorological forcing, soil water content measured in situ at different locations and at multiple soil depths along a hillslope transect, and soil physical and physicochemical properties.

## 2 Site description

The Schäferfetal experimental site is a small headwater catchment (1.44 km<sup>2</sup>) located in the Lower Harz Mountains, in central Germany (51°39' N, 11°3' E). Environmental research at the Schäferfetal catchment was initiated at the end of the 1960s with the implementation of a hydro-meteorological station (Reinstorf et al., 2010), and the infrastructure has continuously been expanded since then. Since 2010, the Schäferfetal catchment is one of the highly instrumented intensive research sites within the TERENO Harz/Central German Lowland Observatory (Zacharias et al., 2011; Wollschläger et al., 2017). Due to the geographical settings of the Harz region, the Schäferfetal catchment receives only 630 mm of precipitation per year. The average annual air temperature is 6.9 °C, with a sub-continental climate (Reinstorf, 2010). The geology of the catchment is dominated by Devonian argillaceous shales and greywackes, covered by periglacial sedi-

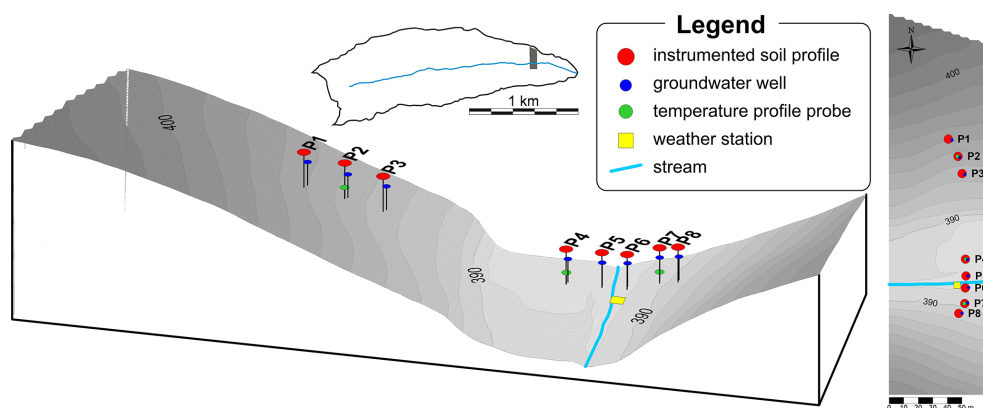


**Figure 1.** Spatial map in 3D and aerial view of the Schäfertal Hillslope site and location of the monitoring stations.

ments (Borchardt, 1982). Near-surface compacted horizons within the basal layer are known to induce interflow processes in the unsaturated zone (Borchardt, 1982; Gräff et al., 2009). Dominant soil types in the Schäfertal are Gleysols occurring in the valley bottom as well as Luvisols and Cambisols on the loess-covered slopes (Ollesch et al., 2005). The slopes of the catchment are intensively used for agriculture, whilst meadows occupy the valley bottom (Schröter et al., 2015).

Since 2012, a smaller hillslope area named Schäfertal Hillslope site, located downstream of the Schäfertal gauging station, has been instrumented for detailed investigations of the hydrological processes in the unsaturated zone. From 2012 to 2017, the wireless soil moisture monitoring network *SoilNet* delivered information about the soil water dynamics at three depths within the unsaturated zone with high spatial coverage. In 2018, the SoilNet was disposed, and a new soil monitoring network, named STH-net, was installed, aiming to improve the resolution in the vertical direction at fewer locations selected based on the knowledge about the soil spatial variability and soil water dynamics gained from the previous monitoring experience (see Martini et al., 2015, 2017a,b). The STH-net is described in the following sections of this paper, and its data are now available through the data portal EUDAT (<https://doi.org/10.23728/b2share.82818db7be054f5eb921d386a0bcaa74>). The Schäfertal Hillslope site includes north- and south-exposed slopes divided by the creek (*Schäferbach*) in the valley bottom (Fig. 1). In contrast to the slopes upstream, which are primarily covered by cropland, this grassland transect is used as pasture and is not affected by agricultural practices except that the grass is mowed typically once per year. The spatial extent of the hillslope is approximately 250 m × 80 m and presents various topographical and pedological features. The slopes are covered by silty loam Cambisols more evolved towards the foot slope, while loam and silty loam stagnic Gleysols occupy the valley bottom. An extensive description of the soil units mapped at the site is provided in Martini et al. (2015). The STH-net is

designed to cover the spatial variability in the soil properties as well as the soil layering with high resolution.

### 3 Monitoring design and measurement techniques

The STH-net comprises eight monitoring stations (named as P1 to P8) arranged along a transect centred within the Schäfertal Hillslope site and aligned along the slope direction (Fig. 1). The stations P1, P2, and P3 are located within the northern (i.e. south-facing) slope and cover the transition between the soil units STU1 and STU2 described in Martini et al. (2015); the stations P4 and P5 fall into the valley bottom, i.e. soil unit STU3; P6, P7, and P8 cover the lower part of the southern (i.e. north-facing) slope, i.e. soil unit STU4. Every station features a soil profile instrumented with time-domain reflectometry (TDR) probes installed every 0.1 m along the vertical direction. A sketch showing the design of a reference monitoring station is presented in Fig. 2. Each of the instrumented soil profiles located on the hillslopes features a minimum of seven TDR probes installed at depths of 0.1, 0.2, 0.3, 0.4, 0.5, 0.6, and 0.7 m, whilst an additional probe is installed at P3 at a depth of 0.8 m, and the profiles at P4 and P5 feature additional TDR probes at depths of 0.8, 0.9, 1.0, and 1.1 m in order to cover the deeper soils. In a few cases, the depths of the probes were adjusted to avoid installing the TDR probe at or too close to the boundaries between soil horizons. The exact depth of every TDR probe is reported in the file “STH-net\_Soils.txt” and displayed in Fig. 3.

At every station, a well instrumented with a piezometer was installed ca. 2 m to the east of the instrumented soil profiles for monitoring the water level. One station for every topographic unit (i.e. northern slope, valley bottom, and southern slope) was further instrumented with sensors measuring the soil temperature at six depths between 0.05 and 1.0 m.

A weather station is located in the centre of the hillslope transect next to the creek.

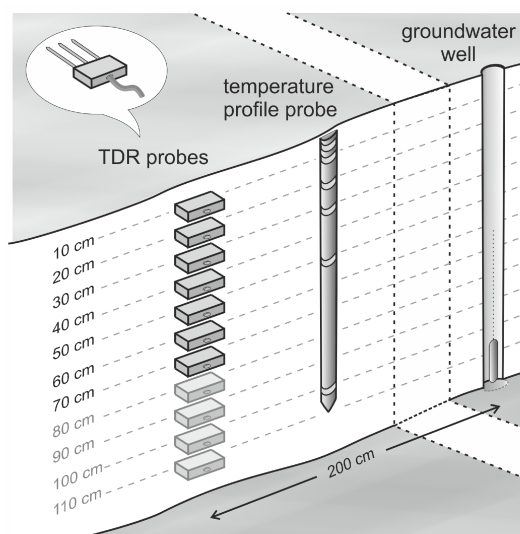


**Figure 2.** Sketch of a representative monitoring station of the STH-net.

All measurement systems comprising the STH-net collect measurements every 10 min, with the only exception of the water level data, which are collected every 2 h.

### 3.1 TDR measurements

The TDR probes are arranged in clusters of 22 probes for the northern slope and the valley bottom, whilst only 21 probes were installed at the southern slope, for a total of 65 TDR probes. Each cluster consists of one TDR device (TDR100 for the station North, TDR200 for the stations Valley and South, Campbell Scientific Inc., Logan, UT, USA) and a data logger (CR1000 for the station North, CR6 for the stations Valley and South, Campbell Scientific Inc., Logan, UT, USA). The clusters are powered by extra-low-voltage cables buried ca. 0.3 m below the ground and cased in HDPE (i.e. high-density polyethylene) tubes and an AGM (i.e. absorbent glass mat) battery capable of supplying the required power in case of power cut-off. Every TDR probe is connected to its station master by a 22 m long low-loss coaxial cable, tested to be the optimal length providing good signal quality while enabling enough flexibility in terms of network design. The TDR probes were custom-made and have three 0.2 m long rods. They were calibrated through measurements in air and in water with different salt concentrations for water content and electrical conductivity estimation. The probes were installed horizontally in soil pits, which were carefully refilled after the installation. The installation was carried out between June and August 2018, and all the measurements collected until the end of December 2018 were discarded to allow the soil to re-compact naturally during the first rainy season.

From the TDR traces, the dielectric permittivity  $\varepsilon$  of the medium is calculated as

$$\sqrt{\varepsilon} = \frac{(\sqrt{\varepsilon_{\text{air}}} - \sqrt{\varepsilon_{\text{water}}})(t - t_{\text{water}})}{t_{\text{air}} - t_{\text{water}}} + \sqrt{\varepsilon_{\text{air}}} \quad (1)$$

based on the calibration measurements of travel time and dielectric permittivity in air ( $t_{\text{air}}$ ,  $\varepsilon_{\text{air}}$ ) and water ( $t_{\text{water}}$ ,  $\varepsilon_{\text{water}}$ ), where  $t$  is the travel time estimated for the measured trace. The volumetric water content  $\theta$  is calculated according to the complex refractive index model (CRIM) following Roth et al. (1990) as

$$\theta = \frac{\sqrt{\varepsilon} - \sqrt{\varepsilon_{\text{soil}}} - \phi(\sqrt{\varepsilon_{\text{air}}} - \sqrt{\varepsilon_{\text{soil}}})}{\sqrt{\varepsilon_{\text{water}}} - \sqrt{\varepsilon_{\text{air}}}}, \quad (2)$$

where  $\phi$  is the porosity, which was calculated from the soil bulk density, and  $\varepsilon_{\text{soil}}$  is set to 4.6. Figure 4 shows the hourly time series of soil water content. Characteristic differences in the soil water dynamics are evident for the distinct soil profiles and depths to be attributed, e.g. to the differences in soil texture and soil layering or, locally, to groundwater dynamics.

### 3.2 Soil temperature

The stations P2, P4, and P7 are instrumented with one Th3-s soil temperature profile probe (formerly UMS GmbH, Munich, Germany) each, located nearby the instrumented soil profiles (Fig. 2) and connected via SDI-12 to the same data loggers and power supply. The probes consist of six temperature sensors cased inside a tube made of glass-fibre-reinforced plastic and placed at fixed depths of 5, 10, 20, 30, 50, and 100 cm. Soil temperature is measured at the same times as the TDR traces. The measured data are shown in Fig. 5. The influence of the geographical exposure of the slopes is particularly evident, e.g. overall higher temperature and stronger dynamics for the south-exposed slopes compared to the other areas as well as the strongest dynamics near the surface compared to the deepest sensors. For every temperature profile, the soil temperature values corresponding to the depths of the TDR profiles within the same cluster (i.e. the same topographic unit, namely northern slope, valley bottom, and southern slope) are calculated based on a linear interpolation and used for calculating the temperature correction of the TDR-measured soil water content values from the TDR traces according to Kaatz (1989). By doing this, we assume that (i) the soil temperature changes linearly with depth between the observations at 5, 10, 20, 30, 50, and 100 cm, regardless of material property changes in-between, and (ii) the soil temperature measured at each of the three plots (i.e. P2, P4, and P7) is representative of the cluster (i.e. cluster North consisting of P1, P2, and P3, measured at P2; cluster Valley consisting of P4 and P5, measured at P4; cluster South consisting of P6, P7, and P8, measured at P7).



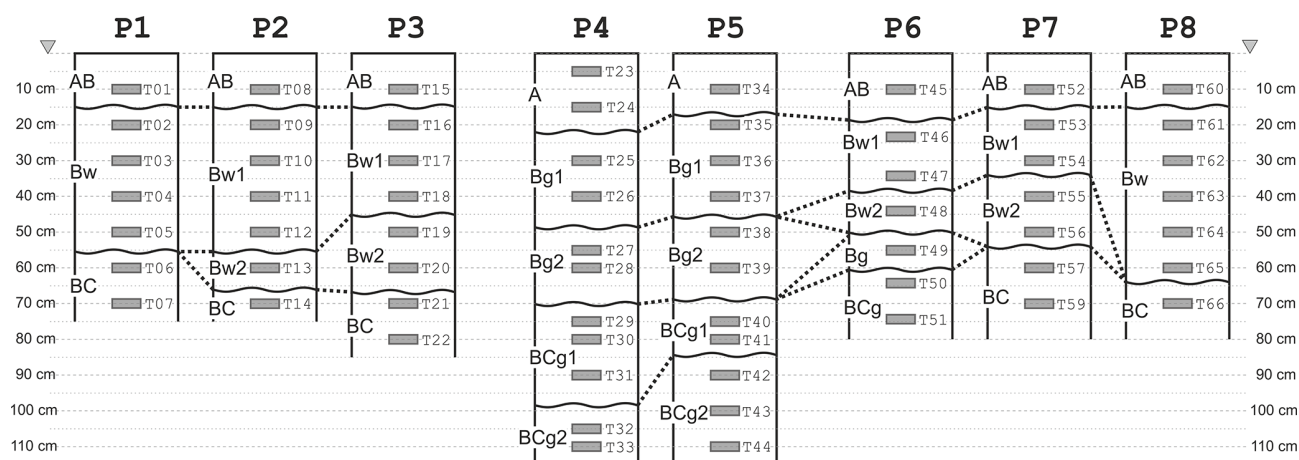


**Figure 3.** Sketch of the soil profiles (showing the mapped soil horizons according to WRB 2015) and the depth of the TDR probes (see labels).

### 3.3 Water level

Every station of the STH-net is equipped with a monitoring well consisting of an LDPE (i.e., low-density polyethylene) tube drilled to the maximum depth of 2 m and instrumented with Levellogger LTC (Solinst, Ontario, Canada), model 3001-M10. Due to an initial malfunctioning of the sensors, only the data measured since 9 March 2020 are available. In contrast to the other measurements of the data set presented here, the water level data are downloaded manually. Figure 6 shows the time series of the water level data and reports the maximum depth for every well. Seasonal dynamics of the groundwater level are evident for the wells in the valley bottom (P4 and P5) and for P6, located next to the creek. The wells on the slopes (P1, P2, P3, P7, and P8) stay dry for most of the monitored period and only show quick rises and recessions of the water level in the winter and spring season.

### 3.4 Meteorological data

In the central part of the Schäferfält Hillslope site (Fig. 1), a WXT 520 weather station (Vaisala Oyj, Laskutus, Finland) equipped with a CMP3-L pyranometer (Kipp & Zonen, Delft, Netherlands) installed at a height of 2 m measures the wind vector, air temperature and pressure, relative humidity, liquid precipitation, hail, and solar radiation. The system is fully integrated with the data logger of the central monitoring station, and the meteorological variables are measured at the same times as the TDR and soil temperature profile probes. Figure 7 shows the hourly time series of the meteorological variables.

### 3.5 Soil properties

During the installation of the STH-net, one bulk soil sample and one volumetric soil sample were collected at every soil

pit at the same depth at which each of the TDR probes were installed. From the bulk samples, the percentage of sand, silt, and clay in the fine earth fraction was determined in the laboratory using the pipette method. The volumetric soil samples were collected with a stainless stain ring and used for the soil porosity and bulk density estimation. Figure 8 shows the classification of the soil samples according to the German soil textural classes (Ad-hoc-AG Boden, 2005), considered suitable for the soil parameterization for physically based hydrological modelling (Bormann, 2007).

## 4 Uncertainties and data usability

For the estimation of soil water content using a composite dielectric approach, some physical parameters must be known. These are primarily temperature, porosity, and the dielectric number of the solid matrix ( $\epsilon_{\text{soil}}$ ). Among them, soil temperature plays a major role in determining the global uncertainty. As part of the STH-net, soil temperature is measured in situ at the same time as the TDR waveforms, which enables an accurate temperature correction. The soil porosity was estimated for every sampling point from undisturbed soil cores and introduces an uncertainty. For  $\epsilon_{\text{soil}}$  we have chosen the value of 4.6, corresponding to the dielectric permittivity of quartz. This value was chosen arbitrarily and hence introduces an uncertainty. For a more extensive discussion about the uncertainty in the soil water content estimation due to the single parameters, we refer to Roth et al. (1990). For the data set presented here, we estimated the uncertainty in the calculated soil water content using the CRIM formula by varying the values of  $\epsilon_{\text{soil}}$  and porosity between 4 and 6 and between 0.3 and 0.5, respectively (similar to Wollschläger et al., 2010). We obtained values  $< \pm 0.03 \text{ m}^3 \text{ m}^{-3}$  as the largest uncertainty in the soil water content estimation. This information is reported in Table 1 along with the measurement

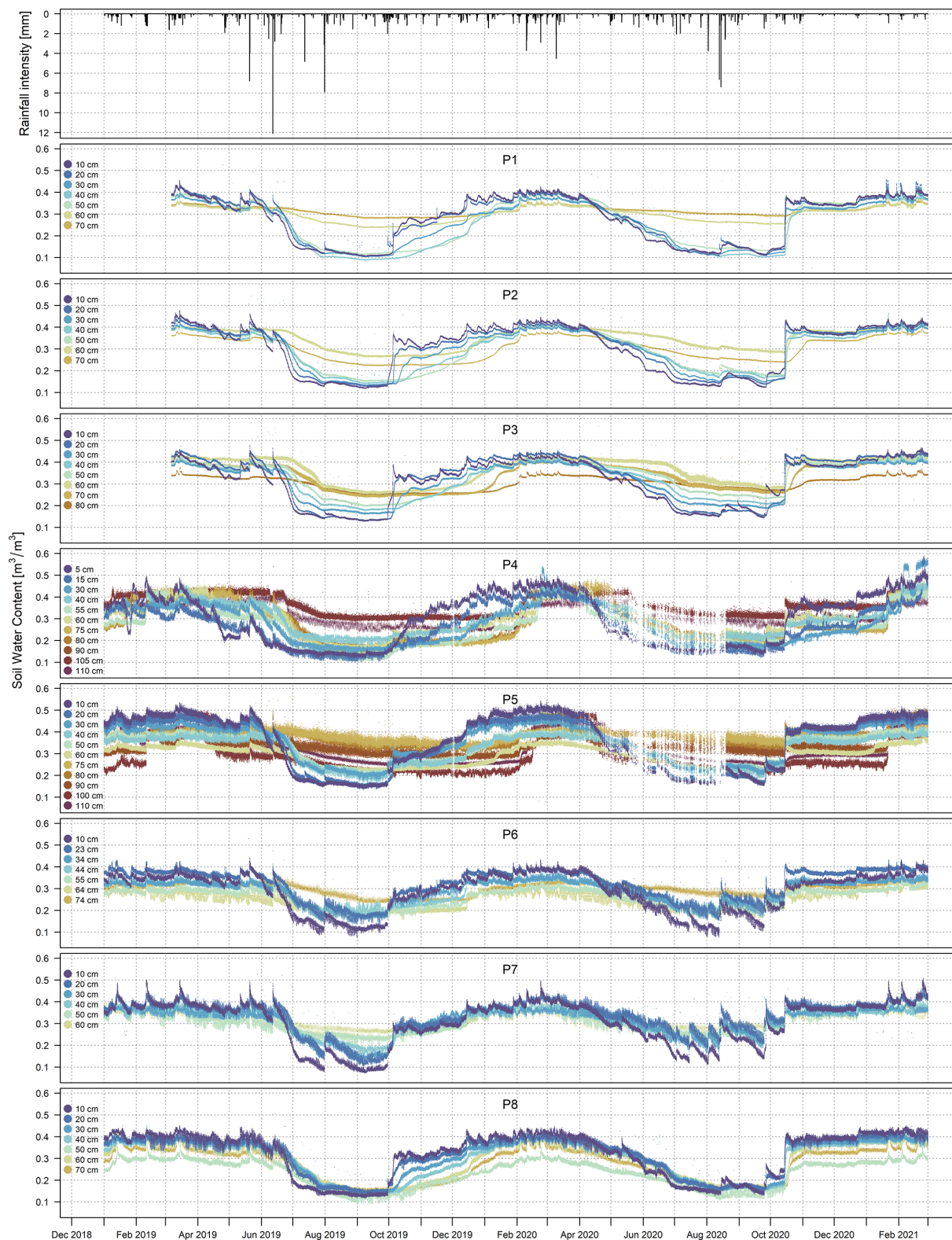


**Figure 4.** Time series of soil water content data. The plots were made using the data set as it appears in the online archive. The data are plotted using a scientific colour scale from Crameri (2018) chosen according to the principles described in Crameri et al. (2020).

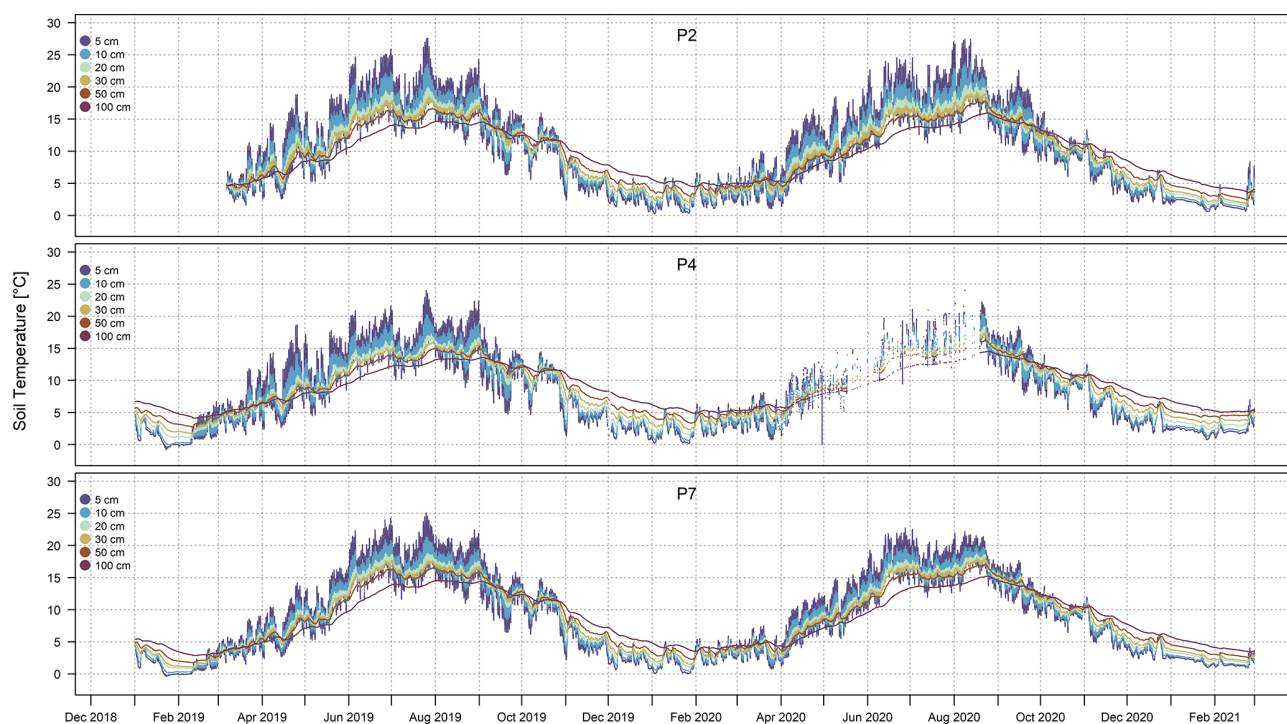


**Figure 5.** Time series of soil temperature data. The plots were made using the data set as it appears in the online archive. The data are plotted using a scientific colour scale from Crameri (2018) chosen according to the principles described in Crameri et al. (2020).

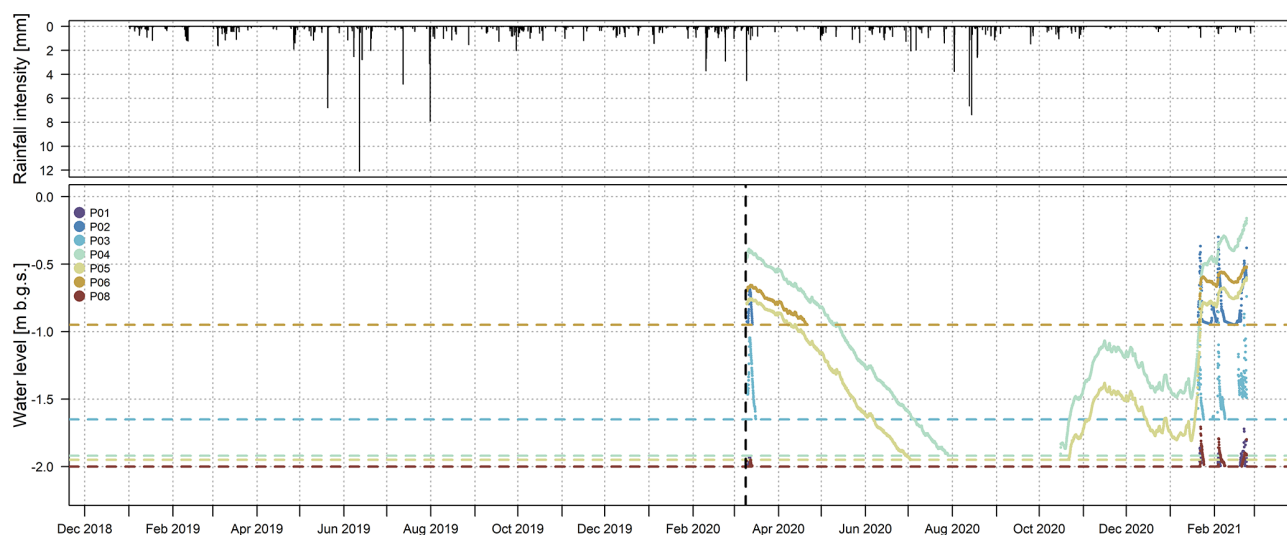


**Figure 6.** Time series of water level data. The plots were made using the data set as it appears in the online archive. The dashed vertical line indicates the start of the measurements (9 March 2020). The dashed horizontal lines indicate the depth of the wells. The data are plotted using a scientific colour scale from Crameri (2018) chosen according to the principles described in Crameri et al. (2020).

range, accuracy, and resolution of the other variables provided within the data set described in this article.

Rain gauges may misestimate the rainfall rate under certain circumstances, especially when rainfall events are associated with strong wind. The experiment described in Basara et al. (2009) shows that a sensor similar to the one installed at

the Schäfertal Hillslope site overestimates the rainfall intensity in an urban environment. The rainfall rate data presented in this article were compared to those of several other rain gauges (data from partner research institute, not available here) located ca. 100 m away from the site. The rainfall intensity values measured by our sensor neither underestimate



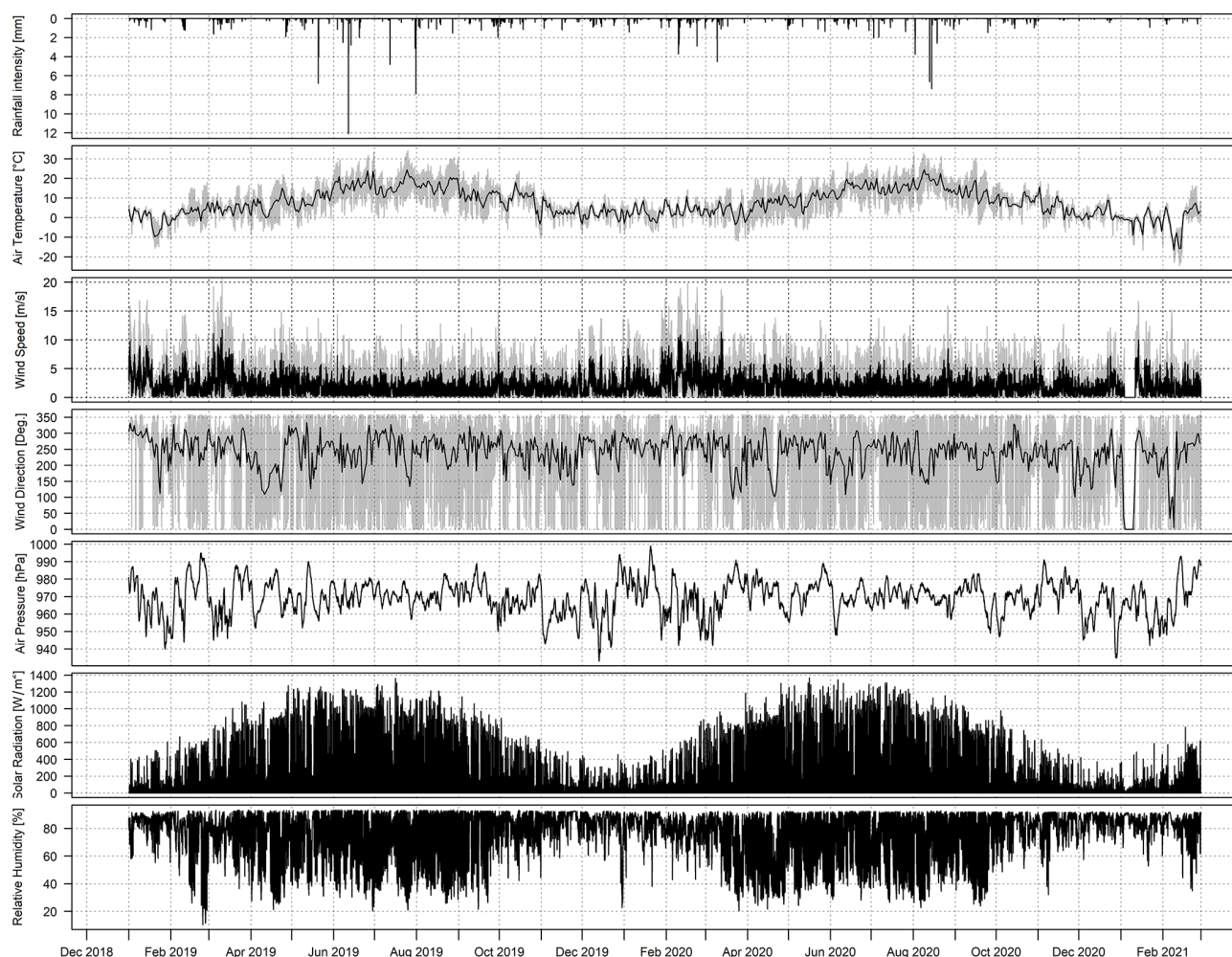


**Figure 7.** Time series of all the meteorological variables measured at the Schäfertal Hillslope site. The plots were made using the data set as it appears in the online archive. The black line in the second, third, and fourth plots shows the daily average temperature, the average wind speed, and the daily average wind direction, respectively, while all other data are in 10 min time steps.

the rainfall rate values nor completely miss rainfall events. With our data set, we make the measured data available to any interested scientists along with all relevant site information and leave them the choice about eventual compensation measures to be applied. The correction function proposed by Richter (1995) is commonly used for studies conducted in central Germany to account for the possible wind-induced underestimation of the rainfall intensity.

Until a few years ago, the Schäfertal catchment used to be affected by significant snowfall, with major snowmelt events occurring between January and April, whose effects on the hydrological processes are described, e.g. in Ollesch et al. (2005). In the last years, however, no significant snowfall events were observed. The last winter period (December 2020 to February 2021), instead, was characterized by exceptionally intense snowfall (with a maximum of ca. 45 cm on 8 February 2021) that accumulated and persisted. Unfortunately, the technical infrastructure currently available at

the site does not allow a meaningful estimation of the snow height and distribution during the monitoring period; hence the snowfall events are not recorded by the weather station in use (see Fig. 7). Because of this, the snow contribution to the water balance needs to be derived from the meteorological and soil temperature data available.

Overall, 9.3 % of the soil water content data and 7.6 % of the soil temperature data are missing (particularly until March 2019 for the station North and between April and August 2020 for the station Valley) due to various technical failures.

## 5 Data management

The STH-net data stored by the three data loggers are accessed and downloaded remotely using the software *Logger-net* (Campbell Scientific Inc., Logan, UT, USA). The water level data, which are manually downloaded, are the only



**Table 1.** Measurement range, accuracy, and resolution of the measurement devices described in Sect. 3.

	Measurement range	Accuracy	Resolution
STH-net station			
Soil water content <sup>1</sup>	0 to 1 m <sup>3</sup> m <sup>-3</sup>	$< \pm 0.03 \text{ m}^3 \text{ m}^{-3}$	NA
Soil temperature <sup>2</sup>	-20 to +50 °C	$\pm 0.1 \text{ °C}$	0.034 °C
Water level <sup>3</sup>	0 to 50 °C (Barologger 5: -10 to +50 °C), FS = 10 m	$\pm 0.5 \text{ cm}$	0.0006 % FS
Weather station			
Barometric pressure <sup>4</sup>	600 to 1100 hPa	$\pm 0.5 \text{ hPa}$ at 0 to +30 °C $\pm 1 \text{ hPa}$ at -52 to +60 °C	0.1 hPa, 10 Pa, 0.001 bar, 0.1 mmHg, 0.01 inHg
Air temperature <sup>4</sup>	-52 to +60 °C	$\pm 0.3 \text{ °C}$	0.1 °C
Wind speed <sup>4</sup>	0 to 60 m s <sup>-1</sup>	$\pm 3 \%$ at 10 m s <sup>-1</sup>	0.1 m s <sup>-1</sup>
Wind direction <sup>4</sup>	0 to 360° azimuth	$\pm 3.0^\circ$	1°
Relative humidity <sup>4</sup>	0 to 100 % RH	$\pm 3 \%$ RH at 0 to 90 % RH $\pm 5 \%$ RH at 90 to 100 % RH	0.1 % RH
Rainfall intensity <sup>4</sup>	0 to 200 mm h <sup>-1</sup> (broader range with reduced accuracy)	Daily accumulation: better than 5 %, weather dependent	0.01 mm
Hail <sup>4</sup>	NA	NA	0.1 hit cm <sup>-2</sup>
Solar radiation <sup>5</sup>	Maximum solar irradiance: 2000 W m <sup>-2</sup>	$\pm 5 \%$	$< \pm 5 \text{ W m}^{-2}$

<sup>1</sup> Custom-made TDR probes (Helmholtz Centre for Environmental Research GmbH – UFZ, Leipzig, Germany). <sup>2</sup> Th3-s soil temperature profile probe (formerly UMS GmbH, Munich, Germany). Source: <https://www.google.com/url?sa=t&rct=j&q=&esrc=s&source=web&cd=&ved=2ahUKEwjQjpTu4bvUahWm4YUKHTKhCsUQFjABegQIARAC&url=http%3A%2F%2Fenhome.cafe24.com%2Fpdf%2FTh3sManual.pdf&usq=AOvVaw1JN8EI6XoJ6F3LyJw9PnnK> (last access: 13 April 2021). <sup>3</sup> 3001-M10 Levellogger LTC (Solinst, Ontario, Canada). Source: <https://www.solinst.com/products/data/3001-ltc.pdf> (last access: 13 April, 2021). <sup>4</sup> WXT 520 weather station (Vaisala Oyj, Laskutus, Finland). Source: <https://www.vaisala.com/en/file/9411/download?token=DOb1ETJK> (last access: 13 April 2021). <sup>5</sup> CMP3-L pyranometer (Kipp & Zonen, Delft, Netherlands). Source: <https://www.kippzonen.com/Product/11/CMP3-Pyranometer> (last access: 13 April 2021). NA – not available

exception. The data files are regularly quality-checked and uploaded to the EUDAT record STH-net (<https://doi.org/10.23728/b2share.82818db7be054f5eb921d386a0bcaa74>, Martini et al., 2020), where they remain available for download.

## 6 Data availability

The STH-net data are available under a dynamic identifier (<https://doi.org/10.23728/b2share.82818db7be054f5eb921d386a0bcaa74>; Martini et al., 2020) at the time of the manuscript submission (from there, all future versions of the archive can be easily accessed) under the Creative Commons Attribution license (CC-BY 4.0).

## 7 Data sets

The STH-net data are archived as separate text files for the different data types: soil water content, soil temperature, water level, and meteorological variables. Furthermore, the geographic coordinates of the measurement locations and the soil information are available for download. The time series data start from 1 January 2019 and continue with hourly time steps until the most recent update. At the time of the manuscript submission, the lat-

est entry refers to 28 February 2021. The water level data are available with a 2 h resolution and cover the time period between 6 March 2020 and 23 February 2021. All the data published in the online archive (<https://doi.org/10.23728/b2share.82818db7be054f5eb921d386a0bcaa74>, Martini et al., 2020) will be updated on an approximately 3-month basis.

**Author contributions.** EM, SK, KR, UIW, UtW, and SZ conceived the work; UIW and SZ acquired the funding; EM, MB, SK, and MK curated the data; EM wrote the manuscript. The joint discussion by all the authors shaped the paper into its actual form.

**Competing interests.** The authors declare that they have no conflict of interest.

**Acknowledgements.** The installation and operation of the Schäfertal Hillslope site research infrastructure was funded and supported by the Terrestrial Environmental Observatories (TERENO), which is a joint collaboration programme involving several Helmholtz Research Centres in Germany, and the TERENO observatory Harz/Central German Lowland operated by the UFZ Helmholtz Centre for Environmental Research is gratefully ac-

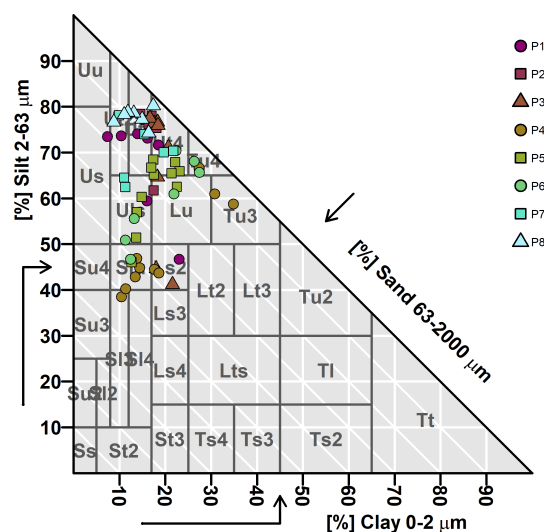


**Figure 8.** Soil textural classification according to the German *Bodenkundliche Kartieranleitung* (Ad-hoc-AG Boden, 2005) grouped by soil profiles (P1 to P8). Ss: pure sand; Su2: slightly silty sand; St2: slightly loamy sand; St3: medium loamy sand; St4: highly loamy sand; Su3: medium silty sand; Su4: highly silty sand; Lu: loamy silty sand; Lt2: slightly clayey loam; Lt3: medium clayey loam; Lt4: highly clayey loam; Ts2: slightly sandy clay; Ts3: medium sandy clay; Ts4: highly sandy clay; Uu: pure silt; Us: sandy silt; Ut2: slightly clayey silt; Ut3: medium clayey silt; Ut4: highly clayey silt; Lu: silty loam; Lt3: medium clayey loam; Tu3: medium silty clay; Ts2: slightly sandy clay; Tu2: slightly silty clay; Tl: loamy clay; Tt: pure clay. The figure was created in RStudio with the package “The Soil Texture Wizard” (<https://CRAN.R-project.org/package=soiltexture>, last access: 1 June 2021) by Julien Moeys. The data are plotted using a scientific colour scale from Crameri (2018) chosen according to the principles described in Crameri et al. (2020).

knowledge for providing access to the Schäfertal Hillslope site and to the STH-net data. Edoardo Martini received funding from the German Research Foundation (DFG).

**Financial support.** This research has been supported by the Deutsche Forschungsgemeinschaft (grant no. MA 7936/1-1).

**Review statement.** This paper was edited by Giulio G. R. Iovine and reviewed by Ian Moffat and six anonymous referees.

## References

Ad-hoc-Arbeitsgruppe Boden: *Bodenkundliche Kartieranleitung*, 5. Aufl., Bundesanstalt für Geowissenschaften und Rohstoffe in Zusammenarbeit mit den Staatlichen Geologischen Diensten, Hannover, 438 pp., ISBN 978-3-510-95920-4, 2005.

- Basara, J. B., Illston, B. G., Winning Jr, T. E., and Fiebrich, C. A.: Evaluation of rainfall measurements from the WXT510 Sensor for use in the Oklahoma City Micronet, *The Open Atmospheric Science Journal*, 3, 39–45, 2009.
- Bauser, H. H., Jaumann, S., Berg, D., and Roth, K.: EnKF with closed-eye period – towards a consistent aggregation of information in soil hydrology, *Hydrol. Earth Syst. Sci.*, 20, 4999–5014, <https://doi.org/10.5194/hess-20-4999-2016>, 2016.
- Bauser, H. H., Riedel, L., Berg, D., Troch, P. A., and Roth, K.: Challenges with effective representations of heterogeneity in soil hydrology based on local water content measurements, *Vadose Zone J.*, 19, e20040, <https://doi.org/10.1002/vzj2.20040>, 2020.
- Borchardt, D.: Geoökologische Erkundung und hydrologische Analyse von Kleinzugsgebieten des unteren Mittelgebirgsbereichs, dargestellt am Beispiel der oberen Selke, Harz, Petermann. *Geogr. Mitt.*, 82, 251–262, 1982.
- Bormann, H.: Analysis of the suitability of the German soil texture classification for the regional scale application of physical based hydrological model, *Adv. Geosci.*, 11, 7–13, <https://doi.org/10.5194/adgeo-11-7-2007>, 2007.
- Botto, A., Belluco, E., and Camporese, M.: Multi-source data assimilation for physically based hydrological modeling of an experimental hillslope, *Hydrol. Earth Syst. Sci.*, 22, 4251–4266, <https://doi.org/10.5194/hess-22-4251-2018>, 2018.
- Bronstert, A.: Capabilities and limitations of detailed hillslope hydrological modelling, *Hydrol. Process.*, 13, 21–48, [https://doi.org/10.1002/\(SICI\)1099-1085\(199901\)13:1<21::AID-HYP702>3.0.CO;2-4](https://doi.org/10.1002/(SICI)1099-1085(199901)13:1<21::AID-HYP702>3.0.CO;2-4), 1999.
- Clark, M. P., Bierkens, M. F. P., Samaniego, L., Woods, R. A., Uijlenhoet, R., Bennett, K. E., Pauwels, V. R. N., Cai, X., Wood, A. W., and Peters-Lidard, C. D.: The evolution of process-based hydrologic models: historical challenges and the collective quest for physical realism, *Hydrol. Earth Syst. Sci.*, 21, 3427–3440, <https://doi.org/10.5194/hess-21-3427-2017>, 2017.
- Crameri, F.: Scientific colour maps, *Zenodo*, <https://doi.org/10.5281/zenodo.1243862>, 2018.
- Crameri, F., Shephard, G. E., and Heron, P. J.: The misuse of colour in science communication, *Nat. Commun.*, 11, 5444, <https://doi.org/10.1038/s41467-020-19160-7>, 2020.
- Fan, Y., Clark, M., Lawrence, D. M., Swenson, S., Band, L. E., Brantley, S. L., Brooks, P. D., Dietrich, W. E., Flores, A., Grant, G., Kirchner, J. W., Mackay, D. S., McDonnell, J. J., Milly, P. C. D., Sullivan, P. L., Tague, C., Ajami, H., Chaney, N., Hartmann, A., Hazenberg, P., McNamara, J., Pelletier, J., Perket, J., Rouholahnejad-Freund, E., Wagener, T., Zeng, X., Beighley, E., Buzan, J., Huang, M., Livneh, B., Mohanty, B. P., Nijssen, B., Safeeq, M., Shen, C., van Verseveld, W., Volk, J., and Yamazaki, D.: Hillslope hydrology in global change research and Earth system modeling, *Water Resour. Res.*, 55, 1737–1772, <https://doi.org/10.1029/2018WR023903>, 2019.
- Gräff, T., Zehe, E., Reusser, D., Lück, E., Schröder, B., Wenk, G., John, H., and Bronstert, A.: Process identification through rejection of model structures in a mid-mountainous rural catchment: observations of rainfall–runoff response, geophysical conditions and model inter-comparison, *Hydrol. Process.*, 23, 702–718, <https://doi.org/10.1002/hyp.7171>, 2009.
- IUSS Working Group WRB: World Reference Base for Soil Resources 2014, Update 2015, World Soil Resources Reports 106, FAO, Rome, ISBN 978-92-5-108369-7, 2015.

- Kaatze, U.: Complex permittivity of water as a function of frequency and temperature, *J. Chem. Eng. Data*, 34, 371–374, <https://doi.org/10.1021/je00058a001>, 1989.
- Martini, E., Wollschläger, U., Kögler, S., Behrens, T., Dietrich, P., Reinstorf, F., Schmidt, K., Weiler, M., Werban, U., and Zacharias, S.: Spatial and temporal dynamics of hillslope-scale soil moisture patterns: characteristic states and transition mechanisms, *Vadose Zone J.*, 14, 1–16, <https://doi.org/10.2136/vzj2014.10.0150>, 2015.
- Martini, E., Werban, U., Zacharias, S., Pohle, M., Dietrich, P., and Wollschläger, U.: Repeated electromagnetic induction measurements for mapping soil moisture at the field scale: validation with data from a wireless soil moisture monitoring network, *Hydrol. Earth Syst. Sci.*, 21, 495–513, <https://doi.org/10.5194/hess-21-495-2017>, 2017a.
- Martini, E., Wollschläger, U., Musolff, A., Werban, U., and Zacharias, S.: Principal component analysis of the spatiotemporal pattern of soil moisture and apparent electrical conductivity, *Vadose Zone J.*, 16, 1–12, <https://doi.org/10.2136/vzj2016.12.0129>, 2017b.
- Martini, E., Kögler, S., Kreck, M., Werban, U., Wollschläger, U., and Zacharias, S.: STH-net, EUDAT, <https://doi.org/10.23728/b2share.82818db7be054f5eb921d386a0bcaa74>, 2020.
- Ollesch, G., Sukhanovski, Y., Kistner, I., Rode, M., and Meissner, R.: Characterization and modelling of the spatial heterogeneity of snowmelt erosion, *Earth Surf. Proc. Land.*, 30, 197–211, <https://doi.org/10.1002/esp.1175>, 2005.
- Reinstorf, F.: Schäferthal, Harz Mountains, Germany. Poster, in: Status and Perspectives of Hydrology in Small Basins, Results and recommendations of the International Workshop in Goslar-Hahnenklee, Germany 2009, and Inventory of Small Hydrological Research Basins, 30 March–2 April 2009, Goslar-Hahnenklee, Germany, edited by: Schumann, S., Schmalz, B., Meesenburg, H., and Schröder, U., available at: [https://www.google.com/url?sa=t&rct=j&q=&esrc=s&source=web&cd=&ved=2ahUKEwjQluqSIMjsAhUOecAKHTnICqsQFjAAegQIAhAC&url=https%3A%2F%2Fwaterandchange.org%2Fwp-content%2Fuploads%2F2017%2F04%2FHeft10\\_en.pdf&usg=AOvVaw2o4w\\_VX74jGiquRs3KaYVR](https://www.google.com/url?sa=t&rct=j&q=&esrc=s&source=web&cd=&ved=2ahUKEwjQluqSIMjsAhUOecAKHTnICqsQFjAAegQIAhAC&url=https%3A%2F%2Fwaterandchange.org%2Fwp-content%2Fuploads%2F2017%2F04%2FHeft10_en.pdf&usg=AOvVaw2o4w_VX74jGiquRs3KaYVR) (last access: 22 October 2020), 2010.
- Richter, D.: Ergebnisse methodischer Untersuchungen zur Korrektur des systematischen Meßfehlers des Hellmann-Niederschlagsmessers, *Berichte des Deutschen Wetterdienstes* 194, Deutscher Wetterdienst, Offenbach am Main, ISBN: 3881483098, available at: <http://nbn-resolving.de/urn:nbn:de:101:1-201601274368> (last access: 1 June 2021), 1995 (in German).
- Roth, K., Schulin, R., Flüßler, H., and Attinger, W.: Calibration of time domain reflectometry for water content measurement using a composite dielectric approach, *Water Resour. Res.*, 26, 2267–2273, <https://doi.org/10.1029/WR026i010p02267>, 1990.
- Schröter, I., Paasche, H., Dietrich, P., and Wollschläger, U.: Estimation of catchment-scale soil moisture patterns based on terrain data and sparse TDR measurements using a Fuzzy C-Means clustering approach, *Vadose Zone J.*, 14, 1–16, <https://doi.org/10.2136/vzj2015.01.0008>, 2015.
- United Nations: Resolution adopted by the General Assembly on 20 December 2013 – 68/232: World Soil Day and International Year of Soils, available at: <https://sdgs.un.org/documents/ares68232-world-soil-day-and-international-year-21058> (last access: 2 June 2021), 60 A/RES/68/232, 2014.
- Vereecken, H., Huisman, J. A., Hendricks Franssen, H. J., Brüggemann, N., Boga, H. R., Kollet, S., Javaux, M., van der Kruk, J., and Vanderborght, J.: Soil hydrology: Recent methodological advances, challenges, and perspectives, *Water Resour. Res.*, 51, 2616–2633, <https://doi.org/10.1002/2014WR016852>, 2015.
- Vereecken, H., Schnepf, A., Hopmans, J. W., Javaux, M., Or, D., Roose, T., J. Vanderborght, Young, M. H., Amelung, W., Aitkenhead, M., Allison, S. D., Assouline, S., Baveye, P., Berli, M., Brüggemann, N., Finke, P., Flury, M., Gaiser, T., Govers, G., Ghezzehei, T., Hallett, P., Hendricks Franssen, H. J., Heppell, J., Horn, J., Huisman, J. A., Jacques, D., Jonard, F., Kollet, S., Lafolie, F., Lamorski, K., Leitner, D., McBratney, A., Minasny, B., Montzka, C., Nowak, W., Pachepsky, Y., Padarian, J., Romano, N., Roth, K., Rothfuss, Y., Rowe, E. C., Schwen, A., Šimůnek, J., Tiktak, A., van Dam, J., van der Zee, S. E. A. T. M., Vogel, H.-J., Vrugt, J. A., Wöhling, T., and Young, I. M.: Modeling Soil Processes: Review, Key challenges and New Perspectives, *Vadose Zone J.*, 15, 1–57, <https://doi.org/10.2136/vzj2015.09.0131>, 2016.
- Vogel, H.-J.: Scale issues in soil hydrology, *Vadose Zone J.*, 18, 1–10, <https://doi.org/10.2136/vzj2019.01.0001>, 2019.
- Vrugt, J. A., Stauffer, P. H., Wöhling, T., Robinson, B. A., and Vesselinov, V. V.: Inverse modeling of subsurface flow and transport properties: A review with new developments, *Vadose Zone J.*, 7, 843–864, <https://doi.org/10.2136/vzj2007.0078>, 2008.
- Wollschläger, U., Pfaff, T., and Roth, K.: Field-scale apparent hydraulic parameterisation obtained from TDR time series and inverse modelling, *Hydrol. Earth Syst. Sci.*, 13, 1953–1966, <https://doi.org/10.5194/hess-13-1953-2009>, 2009.
- Wollschläger, U., Gerhards, H., Yu, Q., and Roth, K.: Multi-channel ground-penetrating radar to explore spatial variations in thaw depth and moisture content in the active layer of a permafrost site, *The Cryosphere*, 4, 269–283, <https://doi.org/10.5194/tc-4-269-2010>, 2010.
- Wollschläger, U., Attinger, S., Borchardt, D., Brauns, M., Cuntz, M., Dietrich, P., Fleckenstein, J. H., Friese, K., Friesen, J., Harpe, A., Hildebrandt, A., Jäckel, G., Kamjunke, N., Knöller, K., Kögler, S., Kolditz, O., Krieg, R., Kumar, R., Lausch, A., Liess, M., Marx, A., Merz, R., Mueller, C., Musolff, A., Norf, H., Oswald, S. E., Rebmann, C., Reinstorf, F., Rode, M., Rink, K., Rinke, K., Samaniego, L., Vieweg, M., Vogel, H.-J., Weitere, M., Werban, U., Zink, M., and Zacharias, S.: The Bode Hydrological Observatory: A platform for integrated, interdisciplinary hydro-ecological research within the TERENO Harz/Central German Lowland Observatory, *Environ. Earth Sci.*, 76, 29, <https://doi.org/10.1007/s12665-016-6327-5>, 2017.
- Zacharias, S., Boga, H., Samaniego, L., Mauder, M., Fuß, R., Pütz, T., Frenzel, M., Schwank, M., Baessler, C., Butterbach-Bahl, K., Bens, O., Borg, E., Brauer, A., Dietrich, P., Hajnsek, I., Helle, G., Kiese, R., Kunstmann, H., Klotz, S., Munch, J. C., Papen, H., Priesack, E., Schmid, H. P., Steinbrecher, R., Rosenbaum, U., Teutsch, G., and Vereecken, H.: A network of terrestrial environmental observatories in Germany, *Vadose Zone J.*, 10, 955–973, <https://doi.org/10.2136/vzj2010.0139>, 2011.